

## Spin-dependent transport of Co-SiO<sub>2</sub> granular films approaching percolation

S. Sankar and A. E. Berkowitz

*Department of Physics and Center for Magnetic Recording Research, University of California—San Diego, La Jolla, California 92093*

David J. Smith

*Department of Physics and Astronomy and Center for Solid State Science, Arizona State University, Tempe, Arizona 85287-1504*

(Received 27 April 2000; revised manuscript received 3 August 2000)

Spin-dependent transport in Co<sub>x</sub>(SiO<sub>2</sub>)<sub>1-x</sub> granular films was investigated just below percolation (volume fraction  $x=0.38, 0.41, 0.46,$  and  $0.50$ ). Co-SiO<sub>2</sub> is an ideal system for investigating magnetic nanoparticle properties since the Co-SiO<sub>2</sub> interfaces are of high quality with no evidence of intermixing, and the saturation magnetization is consistent with bulk values. Transport in these films involves tunneling or hopping. The magnetoresistance is consistent with a spin polarization of 0.26 for the electrons tunneling across the Co-SiO<sub>2</sub> interface, independent of metallic volume fraction and temperature. Ferromagnetic correlations among the Co nanoparticles are evident in the zero-field-cooled (ZFC) state of Co-SiO<sub>2</sub> granular films. For  $x=0.41$ , the correlation is among isolated particles of 40 Å diameter. For  $x=0.46$  and  $0.50$ , at room temperature, there is some ferromagnetic correlation due to dipolar fields from short chains of connected particles. In the ZFC state at 77 K for  $x=0.46$  and  $0.50$ , there are ferromagnetic correlations involving particles that are superparamagnetic at room temperature, similar to the correlation observed for  $x=0.41$  at 77 K.

Granular films, in which magnetic nanoparticles are dispersed in a nonmagnetic matrix, are a very active current research topic because their magnetic and magnetotransport properties suggest some potentially attractive technological applications. These applications include high coercivity films for information storage,<sup>1</sup> high permeability, high resistivity films for shielding and bit writing at high frequencies,<sup>2</sup> and giant magnetoresistance (GMR) for read heads and magnetic sensors.<sup>3</sup> These films also provide convenient systems in which to study the basic properties of magnetic nanoparticles. There are two general types of magnetic granular films—those in which the nonmagnetic matrix is metallic, and those in which the matrix is an insulator. The differences between these two types of systems are substantial.

With a metallic matrix, the nanoparticles and matrix are generally chosen to be immiscible, and the nanoparticles develop by nucleation and growth by homogeneous and heterogeneous modes. The resulting distributions of the nanoparticles' sizes and shapes are generally rather broad. Furthermore, even though the nanoparticles and matrix may be immiscible at equilibrium, there is usually significant mutual solubility when they are prepared by sputtering, deposition, or melt spinning. This introduces difficulties in defining the compositions and boundaries of the nanoparticles and the matrix, which makes analysis of the properties uncertain. Finally, both dipolar and exchange interactions may be present when the matrix is metallic, such as Ruderman-Kittel-Kasuya-Yosida (RKKY) or exchange via a weakly ferromagnetic (FM) matrix, which complicates the analysis of interaction issues.

These problems are largely avoided with an insulating matrix when the tandem deposition method<sup>4</sup> is used, as in the present case. With tandem deposition the metal and insulator are deposited from separate targets onto substrates mounted on a table rotating above the targets. For metallic volume fractions  $<0.5$ , the nanoparticles have a narrow size distribution and are spherical.<sup>4</sup>

For the system discussed in this paper, Co nanoparticles in a SiO<sub>2</sub> matrix, there is no evidence of intermixing since the saturation magnetization is consistent with the amount of Co deposited. Further evidence for clean interfaces is the fact that the inferred spin polarization is temperature independent. Finally, the insulating matrix makes it highly improbable that exchange interactions may be significant. These features make the Co-SiO<sub>2</sub> system well-suited for examining Co nanoparticle systems. We have investigated the magnetoresistance (MR) response in Co-SiO<sub>2</sub> granular films as the metallic volume fraction is increased just below percolation. In this regime, there are strong dipolar interactions that lead to ferromagnetic correlations in the films; these strongly influence the zero-field-cooled (ZFC) MR.

Co<sub>x</sub>(SiO<sub>2</sub>)<sub>1-x</sub> granular films (5000 Å) were cosputtered from separate Co (dc) and SiO<sub>2</sub> (rf) targets onto thermally oxidized Si(100) substrates mounted above on a rotating table. Films for in-line four-probe electrical transport measurements were deposited through shadow masks onto the substrates. The base pressure was  $\sim 3 \times 10^{-7}$  Torr. Deposition was at room temperature in 2 mTorr Ar. The volume fraction  $x$  and total film thickness were determined from calibrated deposition rates. Four compositions,  $x=0.38, 0.41, 0.46,$  and  $0.50$ , will be discussed. The films were structurally characterized with x-ray diffraction (XRD) and transmission electron microscopy (TEM). As deposited, all the films consist of predominantly hcp Co particles that are randomly distributed in an insulating SiO<sub>2</sub> matrix. As noted above and discussed below, Co-SiO<sub>2</sub> is an ideal system from a structural standpoint since the Co-SiO<sub>2</sub> interfaces are of high quality, and there is no evidence of intermixing.

Figure 1 shows a cross-sectional TEM micrograph of a granular film with  $x=0.42$ , as deposited. The darkest contrast corresponds to the Co particles, and the lighter speckled contrast corresponds to the amorphous SiO<sub>2</sub>. The particles

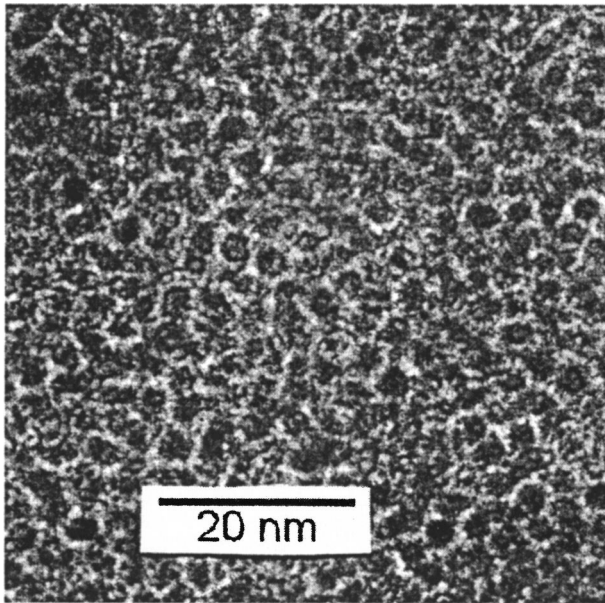


FIG. 1. Cross-sectional TEM micrograph of  $\text{Co}_{42}(\text{SiO}_2)_{58}$ , as deposited. The darkest contrast corresponds to the Co particles ( $\sim 40$  Å in diameter), and the lighter speckled contrast corresponds to the amorphous  $\text{SiO}_2$ .

are about 40 Å in diameter. The average particle volume was also obtained from the zero-field-cooled (ZFC) and field-cooled (FC) dc magnetic susceptibility, measured at 20 Oe using a SQUID magnetometer. As seen in Figs. 2(a) and 2(b), for  $x=0.38$  and 0.41, the ZFC and FC bifurcation temperatures were 65 and 140 K, respectively. As shown in the insets, above the bifurcation temperature, the susceptibility followed a Curie-Weiss behavior, i.e.,  $1/\chi = (3k_B/xM_s^2V)(T - \theta)$ , where  $V$  is the average particle volume. The slope of  $1/\chi$  vs  $T$  in this regime gave particle diameters of 35 and 40 Å for  $x=0.38$  and 0.41, respectively, using the bulk value for  $M_s$ , which are in good agreement with TEM observations. For  $x=0.46$  and 0.50, the bifurcation temperatures are above room temperature, indicating that there are some stable particles at room temperature. Figure 2(c) shows the ZFC and FC data for  $x=0.46$ . From cross-sectional micrographs for  $x\sim 0.50$  and plan-view micrographs of monolayers and discontinuous multilayers,<sup>5</sup> it appears that the increased particle sizes for  $x=0.46$  and 0.50 result from the joining of several Co nanoparticles,  $\sim 40$  Å diameter, into short, randomly oriented chains.

As shown in Fig. 3(a), the resistivity  $\rho(T)$  of the Co-SiO<sub>2</sub> granular films varies as  $\rho_0 \exp\{(T_0/T)^{1/2}\}$ , where  $T_0$  decreases with increasing  $x$ . This temperature dependence was predicted by a model in which charge transport proceeds via thermally activated and/or bias assisted tunneling processes<sup>6</sup> for a system with a distribution of particle sizes and separations. The energy barrier is the Coulomb charging energy  $E_c$  required in creating a pair of charged particles, which is necessary for conduction. The two main assumptions in the model are (1) electrons tunnel between particles of approximately the same size and (2) a uniform composition which implies that  $s/d$  is a constant, where  $s$  is the separation between particles of diameter  $d$ . Assumption (1) results from the fact that an electron cannot tunnel to a smaller particle since the charging energy is larger, whereas a larger particle

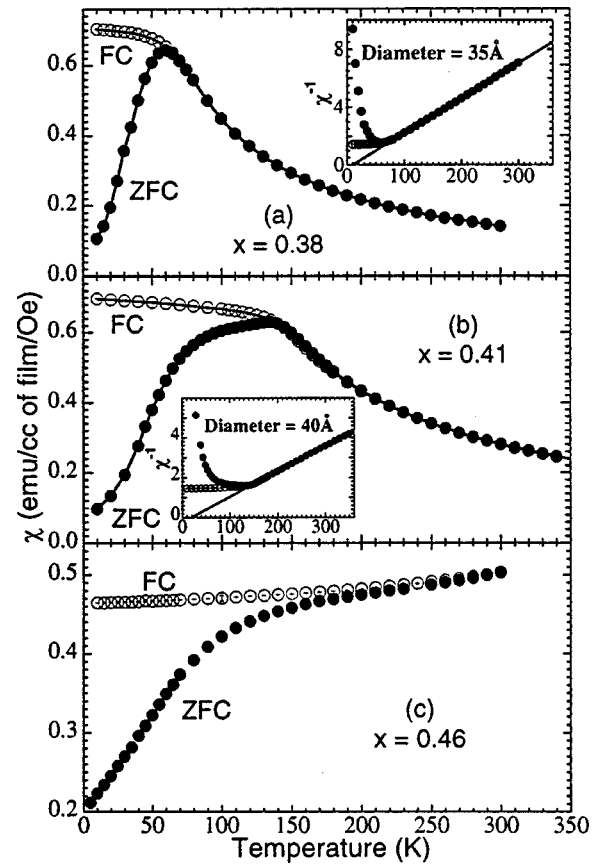


FIG. 2. The zero-field-cooled (ZFC) and field-cooled (FC) dc magnetic susceptibility, measured at 20 Oe using a SQUID magnetometer for granular films with (a)  $x=0.38$ , (b)  $x=0.41$ , and (c)  $x=0.46$ . The insets show the inverse susceptibility; the slopes in the superparamagnetic regime give particle diameters of 35 and 40 Å for  $x=0.38$  and 0.41, respectively.

will be further away and hence the tunnel resistance is larger. From this model the ratio of the particle separation to the particle diameter, i.e.,  $s/d$ , can be directly obtained from  $T_0$ . As shown in Fig. 3(b), the dependence of  $s/d$  on  $x$  is in quantitative agreement of the data with sc packing of the Co particles. However, TEM gives  $s/d$  ratios closer to those for fcc packing. This discrepancy may be accounted for by the fact that the resistivity measurements are sensitive to the smallest values of  $s/d$ . While the ratio of the average values of  $s$  and  $d$ , i.e.,  $\langle s \rangle / \langle d \rangle$ , may be a constant, the particles may have regions where the separation is smallest.

For FM1/insulator/FM2 spin-dependent tunnel junctions (SDTJ's), where FM1 and FM2 are ferromagnetic films, Slonczewski showed that the conductance is proportional to  $\cos \theta$  where  $\theta$  is the angle between the directions of magnetization of the two FM's.<sup>7</sup> Extending the theory to granular films, Inoue and Maekawi showed that the MR of granular films, as defined by  $[\rho(H) - \rho(0)]/\rho(0)$ , is given by  $P^2(M/M_s)^2$  where  $P$  is the polarization of the tunneling electrons.<sup>8</sup> Figure 4 shows the MR and  $(M/M_s)^2$  with a scaling factor for  $\text{Co}_{38}(\text{SiO}_2)_{62}$  at (a) room temperature (RT), and (b) 77 K. The scaling factor gives  $P=0.25$  and 0.26 at RT and 77 K, respectively. The same value of  $P$  was obtained for all the films discussed here. The theoretical polarization<sup>9</sup> of Co is 0.33, and experimental value is 0.35.<sup>10</sup> However,  $P$  is a function of both the FM and barrier mate-

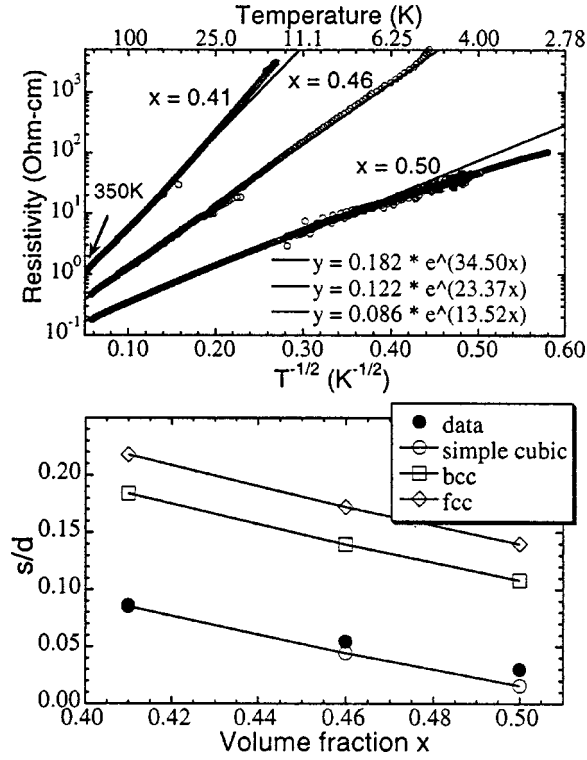


FIG. 3. (a) Temperature dependence of resistivity of  $\text{Co}_x(\text{SiO}_2)_{1-x}$  granular films for  $x=0.41, 0.46,$  and  $0.50$ . The lines are fits to the function  $\rho = \rho_0 \exp\{(T_0/T)^{1/2}\}$ . (b) The ratio of particle separation to particle diameter ( $s/d$ ) obtained from fits of  $\rho(T)$  compared to  $s/d$  calculated for particles on a lattice.

rials, which is not accounted for in the theoretical prediction. In addition, there might be polarization losses due to imperfect metal/insulating interface or due to spin-flip scattering off impurities in the  $\text{SiO}_2$  matrix. However, for SDTJ's imperfect interfaces usually lead to a strong decrease in the MR with increasing temperature,<sup>11</sup> which is not seen for these Co-SiO<sub>2</sub> granular films.

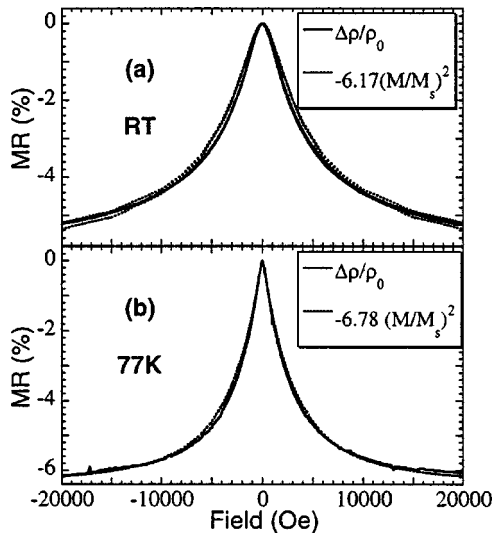


FIG. 4. MR defined as  $[R(H) - R(0)]/R(0)$  and  $(M/M_s)^2$  with a scaling factor for  $\text{Co}_{38}(\text{SiO}_2)_{62}$  at (a) RT, and (b) 77 K. The scaling factors give spin polarization values of 0.25 and 0.26 at RT and 77 K, respectively.

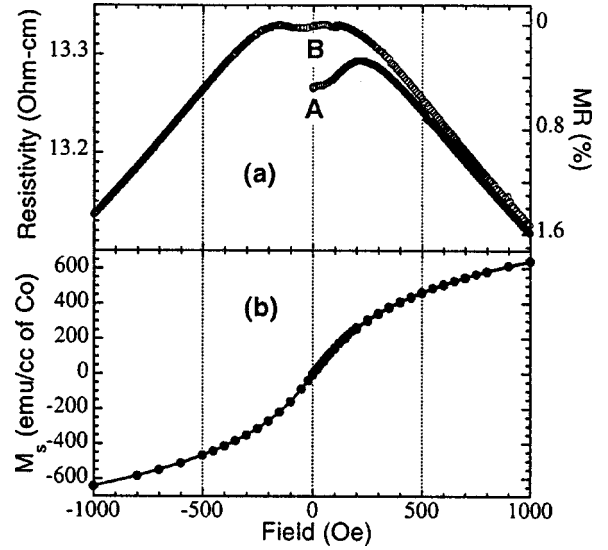


FIG. 5. (a) ZFC resistivity of  $\text{Co}_{41}(\text{SiO}_2)_{59}$  at 77 K. The label A denotes the initial resistance after the ZFC procedure. As the field is increased, the resistance first increases reaching a maximum before decreasing in the normal way. In the reverse sweep direction (and subsequent cycles), the zero field resistance (B) is higher than that at A. (b) Corresponding ZFC  $M(H)$  at 77 K. The initial ZFC  $M(H)$  after the ZFC procedure (zero field) is zero, and the initial  $M(H)$  curve is the same as  $M(H)$  from  $H_{\text{saturation}}$  to 0.

For  $x=0.41$ , in which the particles are all superparamagnetic above 140 K, the ZFC MR at 77 K is consistent with ferromagnetic correlation of isolated particles. The film was cooled to 77 K in zero field, and the resistance was measured by increasing the in-plane magnetic field up to 20 kOe, then sweeping to  $-20$  kOe. Figure 5(a) shows the MR in  $\pm 1000$  Oe. The label A marks the initial resistance after the ZFC procedure. Note that if the particles' magnetizations were uncorrelated, the resistance at A would be the maximum, which is *not* the case. As the field is increased, the resistance first increases to a maximum, and then decreases. In the reverse sweep direction (and subsequent cycles), the zero field resistance (B) is higher than that at A. No corresponding features are seen in the magnetization curves shown in Fig. 5(b). The magnetization after the ZFC procedure is zero, and the initial magnetization curve is the same as  $M(H)$  from  $H_{\text{saturation}}$  to 0. Both curves are plotted in Fig. 5(b) but they are indistinguishable.

The data suggest that in the ZFC state (at A), a fraction of the particles couple ferromagnetically in finite regions with orientation distributions such that the net magnetization is zero, i.e., to reduce the Zeeman energy. The spin-dependent tunneling in ferromagnetically coupled regions gives a low resistance. As the field is increased, the ferromagnetic correlations among the moments of particles within each coupled region are disrupted as particles' moments align along their randomly oriented anisotropy axes or towards the field direction. Initially, this produces more randomness in the magnetization directions of the particles, yielding a maximum in resistance. Then the resistance decreases with increasing field as the particle moments align with the field. In the reverse field from saturation, the zero field resistance (B) is higher than A, which implies that the magnetically correlated state is disrupted by the applied magnetic field. However,

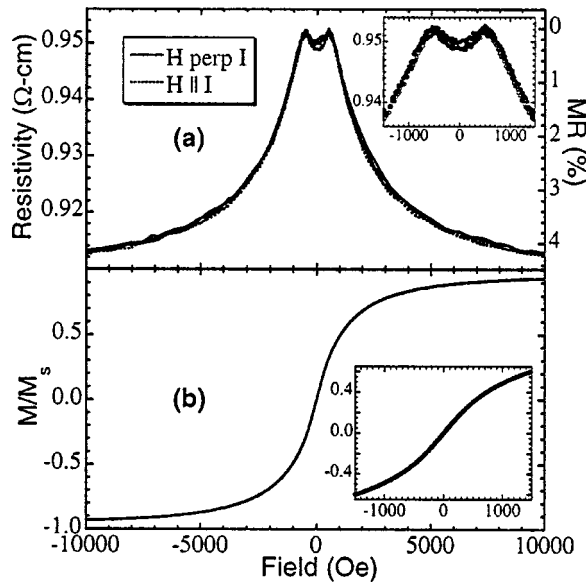


FIG. 6. (a) MR and (b)  $M(H)$  for  $\text{Co}_{46}(\text{SiO}_2)_{54}$ , measured at RT with the current both parallel and perpendicular to the applied field. Inset: Low field response showing anomalous behavior around  $H = 0$  for MR. There is no corresponding feature in  $M(H)$ .

there is evidence of some interactions in this remanent state, suggested by the almost flat MR response within  $\pm 170$  Oe. These results were independent of the relative orientation of the field and current, which, together with the high tunneling resistance, eliminate anisotropic magnetoresistance (AMR)<sup>12</sup> as the origin of the observed behavior. The magnetic order in the ZFC state was investigated with small angle neutron scattering (SANS), and an antiferromagnetic periodicity of 1100 Å was found for magnetically correlated regions<sup>13</sup> in this sample.

For  $x=0.46$  and  $0.50$ , the MR exhibits an anomalous behavior in low magnetic fields at RT, similar to that observed in CoFe-AgCu metallic composite films. However, the training effect observed these metallic films is not observed here.<sup>14</sup> Figure 6(a) shows the MR at RT for  $x=0.46$  measured with the current perpendicular and parallel to the applied field. The most striking feature in the MR curves is the local minimum at  $H=0$ . There are no corresponding features in  $M(H)$ , plotted in Fig. 6(b). Since the MR data are the same for current perpendicular and parallel to the applied field, even at the maximum field of 20 kOe, the feature is not due to AMR. Furthermore, the sample exhibits a resistivity compatible with tunneling ( $0.62 \Omega \text{ cm}$ ), whereas AMR is on the order of metallic resistivity ( $10^{-5} \Omega \text{ cm}$ ). The MR at 300 K for  $x=0.46$  bears some similarity to the MR at 77 K for  $x=0.41$  in that the zero-field resistance is not a maximum. Thus, it is possible that the low field effect for  $x=0.46$  is also due to ferromagnetic interactions. Thus, as the field is reduced to zero, particles separated by a tunneling resistance couple ferromagnetically in finite regions such that the net magnetization is zero. In general, magnetic interactions are expected to increase with increasing volume fraction since the particle sizes are larger and the separation is smaller. Thus, it is not surprising that we should see features due to magnetic interactions at higher temperature for  $x=0.46$  than for  $0.41$ . Zero-field-cooled experiments to investigate this hypothesis are discussed below. An explanation based on

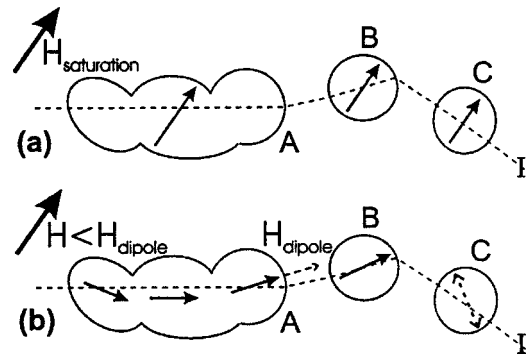


FIG. 7. Model to explain low-field MR response for  $x=0.46$ . (a) Minimum resistance at saturation (b) At zero low field, A becomes magnetized along its length due to a large shape anisotropy, and the dipolar field due to A leads to a ferromagnetic correlation between A and B. Thus, the tunneling resistance between A and B is not as high as it should be if they were uncorrelated or in fields larger than  $H_{\text{dipole}}$ .

magnetic interactions was also proposed to explain the magnetic domains seen in metallic CoFe-AgCu metallic composite films.<sup>14,15</sup> However, in that case, a combination of a weakly ferromagnetic matrix, an unknown distribution of particles and a uniaxial anisotropy perpendicular to the film plane, led to stripe or bubble domains in that system. This is quite different from the Co-SiO<sub>2</sub> films in which the only interactions, as described above, are dipolar interactions, and the moments are primarily in the plane. Thus, we propose an alternate explanation of our result.

A plausible mechanism to explain the low-field MR data for  $x=0.46$  is illustrated in Fig. 7. The feature is that short chains consisting of few particles, as observed in TEM micrographs, are responsible for the effect. The presence of these chains is consistent with the bifurcation temperature of the ZFC and FC susceptibility appearing above 350 K. The current through the film will choose the path of lowest resistance, which implies that the current will always flow along the length of the chains and out of the ends into the closest particles. Therefore, a current path such as illustrated in Fig. 7 will influence the resistance. In a large applied field, the magnetization of all the particles (A–C) is saturated in the field direction, as illustrated in Fig. 7(a), which is a low resistance state. As the field is reduced, the magnetization of each particle rotates along its easy axis due to their individual anisotropy, so the resistance increases. For particles B and C, the anisotropy is magnetocrystalline, whereas for A it is due to shape. As the chain A becomes magnetized along its length, as illustrated in Fig. 7(b), the dipolar fields at the ends increase, and at some point, the dipolar field from A influencing particle B is stronger than the applied field. In zero applied field, the dipolar field  $H_{\text{dipole}}$ , due to particle A induces a ferromagnetic correlation between A and B. Thus, the tunneling resistance between A and B is not as high as it would be if they were uncorrelated. The interaction between A and B at room temperature is most likely short ranged and affects only a small number of particles since the effect is small. Most of the tunneling in the film may still be between superparamagnetic particles such as particle C.

For  $x=0.50$ , as shown in Fig. 8(a), the low field MR response is more complicated. As with  $x=0.41$  and  $0.46$ ,

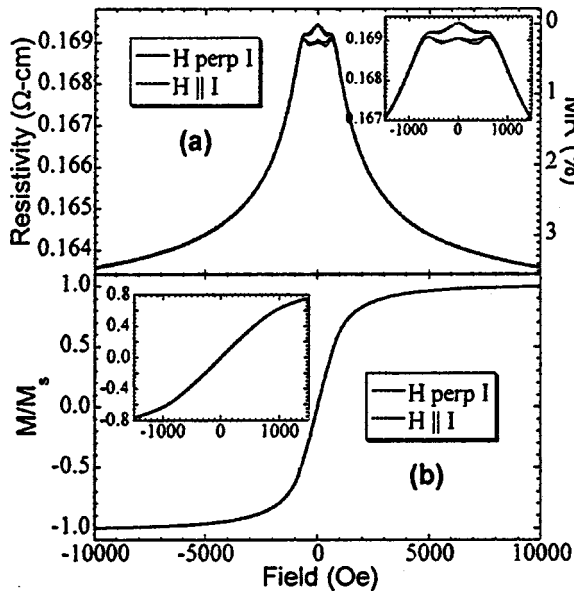


FIG. 8. (a) MR and (b)  $M(H)$  for  $\text{Co}_{50}(\text{SiO}_2)_{50}$ , measured at RT with the current both parallel and perpendicular to the applied field. Inset: Low field response showing anomalous behavior around  $H = 0$  for MR. There is no corresponding feature in  $M(H)$ .

there are no corresponding features in  $M(H)$ , shown in Fig. 8(b). However, in this case, there is a difference at low fields for the current perpendicular and parallel to the applied field. The effect again does not appear to be due to AMR since the magnitude of the saturation resistance is independent of the relative orientation of the field and current. The local minima at low field and maximum at zero field may be explained by ferromagnetic and antiferromagnetic correlation developing in the film as the field is reduced from saturation. The different zero-field resistances for the field perpendicular and parallel to the current indicate that the remanent magnetic structure is different for the two cases. However, in both cases the net magnetic moment is zero, as seen in Fig. 8(b). The different magnetic structures between current perpendicular and parallel to the applied field might be due to an anisotropy in the film, since for the MR measurements, the current direction was fixed and the field was rotated by  $90^\circ$ . A very weak uniaxial in-plane anisotropy of  $\sim 2000$  ergs/cc of Co was measured by torque magnetometry and observed in SANS for  $x=0.41$ . This anisotropy for  $x=0.41$  could not be detected by bulk magnetic or MR measurements. Figure 9 shows the initial MR curves for  $x=0.50$  after demagnetizing the sample for (a) the current perpendicular to the applied and (b) the current parallel to the applied field. The initial MR for both cases (A and A') is the same. However, the field dependence is quite different, and consistent with Fig. 8 and the presence of a weak anisotropy.

When the films with  $x=0.46$  and  $0.50$  are cooled in zero field to 77 K, the MR response is similar to that observed for  $x=0.41$ . Figure 10 shows the ZFC MR for (a)  $\text{Co}_{46}(\text{SiO}_2)_{54}$  and (b)  $\text{Co}_{50}(\text{SiO}_2)_{50}$ . The label A marks the initial resistance after the ZFC procedure and the label B marks the maximum resistance. Note that since there is some coercivity in the films, the maximum resistance is not at zero field, but at the coercive field. Compared to  $x=0.41$ , the difference in resis-

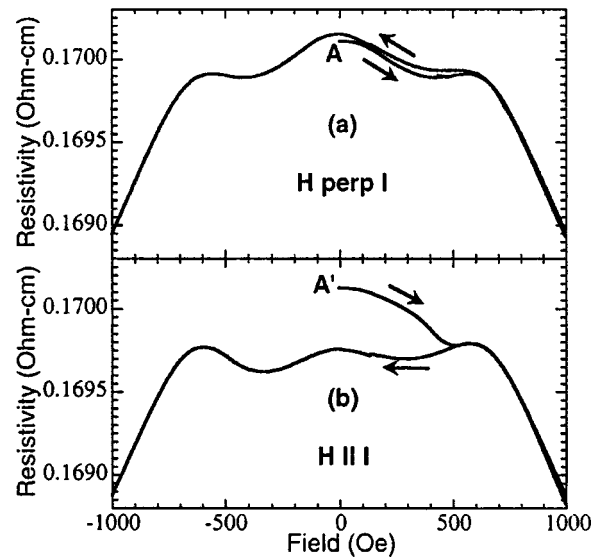


FIG. 9. Initial MR and MR curve of  $\text{Co}_{50}(\text{SiO}_2)_{50}$ , measured at 300 K with (a) current perpendicular to the applied field and (b) current parallel to the applied field. The initial resistances for both cases (A and A') are the same.

tance of A and B is much larger; for  $x=0.46$  and  $0.50$  it is approximately 40% of the total MR, as compared to 12% for  $x=0.41$ . Figure 11 shows  $M(H)$  for these two films. The data were taken in  $\pm 50$  kOe but plotted for  $\pm 1000$  Oe to show the low field behavior. After the ZFC procedure, the magnetization is zero for both films. Thus, as found for  $x=0.41$ , in the ZFC state (at A), the particles couple ferromagnetically in finite regions such that the net magnetization is zero. However, the coupled regions for  $x=0.46$  and  $0.50$  are much larger than those for  $x=0.41$  since the effect is so

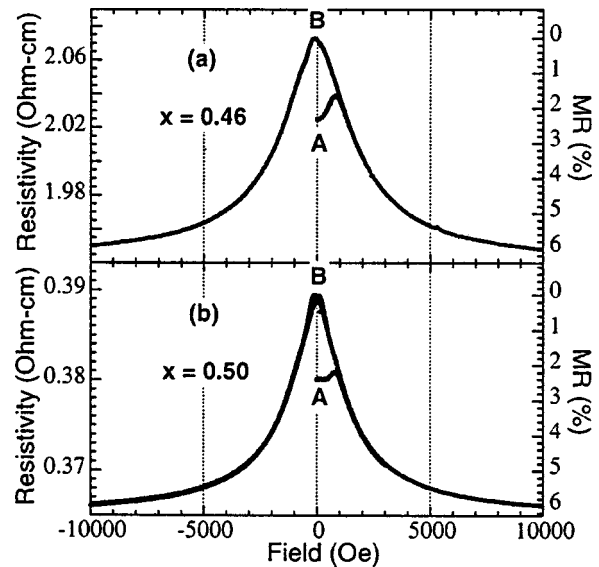


FIG. 10. ZFC MR of (a)  $\text{Co}_{46}(\text{SiO}_2)_{54}$  and (b)  $\text{Co}_{50}(\text{SiO}_2)_{50}$ . The label A marks the initial resistance after the ZFC procedure. As the field is increased, the resistance first increases to a maximum, and then decreases. In the reverse sweep direction (and subsequent cycles), the zero field resistance (B) is higher than that at A. The difference in resistance of A and B is approximately 40% of the total MR.

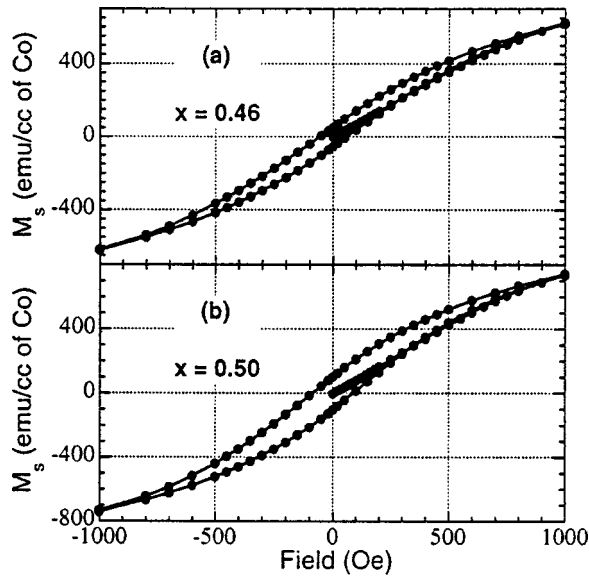


FIG. 11. ZFC  $M(H)$  of (a)  $\text{Co}_{46}(\text{SiO}_2)_{54}$  and (b)  $\text{Co}_{50}(\text{SiO}_2)_{50}$ . For both films,  $M(0)$  after the ZFC procedure is zero. There are no features corresponding to those in the MR data.

much larger. The particles that are involved in the ordering are separated by tunneling resistances since they contribute to a large part of the magnetoresistance, and the resistance was shown to be due to a tunneling or hopping mechanism from the temperature dependence in Fig. 3. From Fig. 8, the 40% decrease in resistance of the ZFC state at 77 K implies that particles that are superparamagnetic at room temperature become ferromagnetically correlated in the ZFC state at 77 K. We note also that the correlations in the ZFC state are disrupted by large fields, and the magnetic state obtained after decreasing the field from saturation to the coercivity is

different from the ZFC state. In other words, ZFC state is a metastable low, energy state.

Finally, once the film is saturated at 77 K and the field swept as in a normal hysteresis loop, the  $\text{MR} \propto (M/M_s)^2$ . The MR ratio is similar to that for  $x=0.38$  and  $0.41$ , and the scaling factors of  $(M/M_s)^2$  give polarization values of 0.251 and 0.253 for  $x=0.46$  and  $0.50$ , respectively. These are in agreement with the polarization values obtained for  $x=0.38$  and  $0.41$ , as shown in Fig. 4.

In conclusion, we have investigated the transport and spin-dependent transport of  $\text{Co-SiO}_2$  granular films just below percolation. For all the films discussed, the resistance is due to tunneling or hopping conductivity. The magnetoresistance is consistent with a polarization of 0.26 for the electrons tunneling across the  $\text{Co-SiO}_2$  interfaces, independent of metallic volume fraction and temperature. Ferromagnetic correlations among groups of the Co nanoparticles, due to dipolar interactions, are evident in the ZFC state of the  $\text{Co-SiO}_2$  granular films. In the correlated state the net magnetic moment is zero. For  $x=0.41$ , the correlation is among isolated particles of 40 Å diameter. For  $x=0.46$  and  $0.50$ , at room temperature, there is some ferromagnetic correlation due to dipolar fields from short chains of connected particles. This involves only a small fraction of nearest neighbors, since the change in resistance due to this effect is very small. In addition, in the ZFC state for  $x=0.46$  and  $0.50$ , there is ferromagnetic correlation involving particles that are superparamagnetic at room temperature, similar to the correlation observed for  $x=0.41$ . The difference between the ZFC resistance and the maximum resistance is about 40% of the total MR for these volume fractions, implying that the magnetic correlation scale is considerable larger than that observed for  $x=0.41$  in which the corresponding MR difference is only 12%.

- <sup>1</sup>S. Stavroyiannis, I. Panagiotopoulos, D. Niarchos, J. A. Christodoulides, Y. Zhang, and G. Hadjipanayis, *J. Appl. Phys.* **85**, 4304 (1999); M. Yu, Y. Liu, A. Moser, D. Weller, and D. J. Sellmeyer, *Appl. Phys. Lett.* **75**, 3992 (1999); M. Watanabe, T. Masumoto, D. H. Ping, and K. Hono, *ibid.* **76**, 3971 (2000).
- <sup>2</sup>S. Ohnuma, H. Fujimori, S. Mitani, and T. Masumoto, *J. Appl. Phys.* **79**, 5130 (1996); T. Morikawa, M. Suzuki, and Y. Taga, *J. Magn. Soc. Jpn.* **23**, 234 (1999).
- <sup>3</sup>S. Mitani, H. Fujimori, K. Takanashi, K. Yakushiji, J.-G. Ha, S. Takahashi, S. Maekawa, S. Ohnuma, N. Kobayashi, T. Masumoto, M. Ohnuma, and K. Hono, *J. Magn. Mater.* **198-199**, 179 (1999).
- <sup>4</sup>E. M. Logothetis, W. J. Kaiser, H. K. Plummer, and S. S. Shinzaki, *J. Appl. Phys.* **60**, 2548 (1986).
- <sup>5</sup>David J. Smith and S. Sankar (unpublished).
- <sup>6</sup>P. Sheng, B. Abeles, and Y. Arie, *Phys. Rev. Lett.* **31**, 44 (1973); B. Abeles, P. Sheng, M. D. Coutts, and Y. Arie, *Adv. Phys.* **24**, 407 (1975).
- <sup>7</sup>J. C. Slonczewski, *Phys. Rev. B* **39**, 6995 (1989).
- <sup>8</sup>J. Inoue and S. Maekawa, *Phys. Rev. B* **53**, R11 927 (1996).
- <sup>9</sup>M. B. Stearns, *J. Magn. Mater.* **5**, 167 (1977).
- <sup>10</sup>R. Meservey and P. M. Tedrow, *Phys. Rep.* **238**, 174 (1994).
- <sup>11</sup>T. Miyazaki and N. Tezuka, *J. Magn. Mater.* **151**, 403 (1995); Y. Lu *et al.*, *J. Appl. Phys.* **83**, 6515 (1998).
- <sup>12</sup>T. G. S. M. Ryks, S. K. J. Lenczewski, R. Coehoorn, and W. J. M. De Jonge, *Phys. Rev. B* **56**, 362 (1997).
- <sup>13</sup>S. Sankar, D. Dender, J. A. Borchers, D. J. Smith, R. W. Erwin, S. R. Kline, and A. E. Berkowitz, *J. Magn. Mater.* **221**, 1 (2000).
- <sup>14</sup>V. Franco, X. Battle, and A. Labarta, *J. Appl. Phys.* **85**, 7328 (1999).
- <sup>15</sup>V. Franco, X. Battle, A. Valencia, A. Labarta, K. O'Grady, and M. L. Watson, *IEEE Trans. Magn.* **34**, 912 (1998).